Supplementary material: Why graphene growth is very different on the C face than on the Si face of SiC: Insights from surface equilibria and the (3×3)-*3C*-SiC($\bar{1}\bar{1}\bar{1}$) reconstruction

Lydia Nemec,[1] Florian Lazarevic,[1,*] Patrick Rinke,[1,2] Matthias Scheffler,[1] and Volker Blum[3,1]

[1] *Fritz-Haber-Institut der Max-Planck-Gesellschaft, D-14195, Berlin, Germany*
[2] *COMP/Department of Applied Physics, Aalto University, P.O. Box 11100, Aalto FI-00076, Finland*
[3] *Department of Mechanical Engineering and Material Science, Duke University, NC 27708 USA*

(Dated: April 15, 2015)

Methodology

The FHI-aims code employs numeric atom-centered basis sets; basic descriptions of their mathematical form and properties are published in [1]. The chosen basis set and numerical real space grids are of high quality as defined by the *tight* settings including for Si a *tier* 1+dg and for C a *tier* 2 basis set [1]. All surface structures are calculated using a slab of six SiC bilayers. The bottom silicon atoms are hydrogen terminated. The top three SiC bilayers and all adatoms or planes above are fully relaxed (residual energy gradients: $8 \cdot 10^{-3}$ eV/Å or below). For accurate integrations in reciprocal space, we chose the (3×3) reconstructions a $4 \times 4 \times 1$ k-mesh, for the $(2\times2)_C$ a $6 \times 6 \times 1$ k-mesh and for the $(6\sqrt{3} \times 6\sqrt{3})$ interfaces the Γ-point.

In a previous work, we included in the supplemental material (SM) details about the numerical convergence with respect to the grid density in real- and reciprocal space and number of basis functions, and we showed the effect of zero-point corrections on the reference bulk phases for different functionals [2].

In this work, we used the Heyd-Scuseria-Ernzerhof hybrid functional (HSE06)[3] for calculating the electronic structure and validating surface energies. In HSE06 the amount of exact exchange is set to $\alpha = 0.25$ and the range-separation parameter $\omega = 0.2\text{Å}^{-1}$. As can be seen in Fig. 1, for fixed (ω) the band gap and valence band width depend practically linearly on the exchange parameter α. We tested the HSE06 with respect to the band gap and band width, the latter being a measure for the cohesive properties of a crystal[6]. The default HSE06 value of $\alpha = 0.25$ captures both the band gap and the band width well and we therefore adopt it for our calculations.

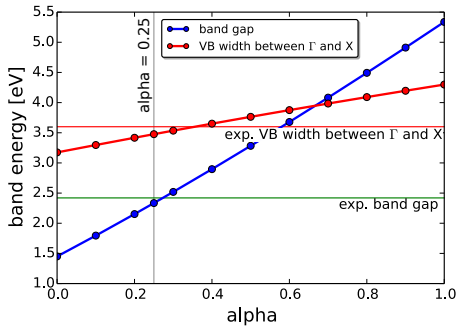

FIG. 1: The Kohn-Sham band-gap (blue circles) and valence band width along Γ to X (red circles) of *3C*-SiC as a function of α. The HSE06 value $\alpha = 0.25$ is marked by a vertical line. The experimental valence band width is shown as horizontal line at 3.6 eV[4] and the exp. band gap at 2.42 eV[5]. The lattice paramter listed in Tab. I for HSE06+vdW were used.

Bulk structure and enthalpy of formation of *3C*-SiC, diamond, graphite and silicon

For all calculations included in this work we used fully relaxed (locally optimized) atomic structures. We here list the optimised lattice parameters a_0 [Å] and the resulting enthalpy of formation ΔH_f [eV] for *3C*-SiC and the cohesive energies of the reference structures diamond, graphite and silicon and *3C*-SiC. The lattice parameter without zero-point vibrational corrections (ZPC) and the cohesive energies are listed in Tab. I, the influence of ZPC is given in the SM of Ref. [2]. The enthalpy of formation ΔH_f is calculated for bulk silicon and carbon in the diamond structure as the reference phases. ΔH_f is −0.56 eV for PBE+vdW and −0.59 eV for HSE06+vdW. ΔH_f shows good agreement with the previously obtained values calculated within the random phase approximation (RPA) $\Delta H_f = -0.66$ eV [8] and using HSE03[9]

		PBE+vdW	HSE06+vdW
Graphite	a_0, c_0 [Å]	2.46, 6.66	2.44, 6.64
	E_{coh} [eV/atom]	-8.00	-7.78
Diamond	a_0 [Å]	3.55	3.53
	E_{coh} [eV/atom]	-7.93	-7.76
Silicon	a_0 [Å]	5.45	5.43
	E_{coh} [eV/atom]	-4.87	-4.82
3C-SiC	a_0 [Å]	4.36	4.34
	E_{coh} [eV/atom]	-6.76	-6.59
	ΔH_f [eV]	-0.56	-0.59

TABLE I: Lattice parameter a_0 and c_0 and cohesive energies E_{coh} for graphite, diamond and silicon in diamond structure and *3C*-SiC as obtained in this work. The experimental lattice parameter of *3C*-SiC is 4.36 Å [7]. The enthalpy of formation ΔH_f of *3C*-SiC is given.

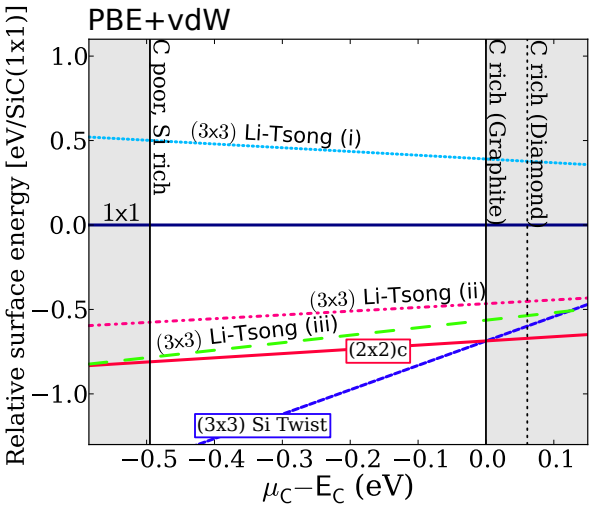

FIG. 2: Comparison of the surface energies for three different chemical compositions of the tetrahedrally shaped cluster as adatoms forming the *3C*-SiC($\bar{1}\bar{1}\bar{1}$)-(3×3) reconstruction. The surface energies are given relative to the bulk-truncated (1×1) phase, as a function of the C chemical potential within the allowed ranges (given by diamond Si, diamond C or graphite C, respectively), using the graphite limit as zero reference. In addition, the known $(2\times2)_C$ reconstruction and the (3×3) Si twist model are shown.

−0.66 eV including zero-point corrections or an experimental value of −0.77 eV [10].

The atomic structure of *3C*-SiC($\bar{1}\bar{1}\bar{1}$)-(3×3) reconstructions

Figure 4 shows the atomic structure of various alternative surface phases of the SiC C-face that have been proposed in the literature[11–14]. First the *Si twist model*, which has been adapted from the Si face [15], is shown in Fig. 4 *a* and discussed in the main paper. As can be seen in Fig. 4 *b*, the $(2\times2)_C$ reconstruction as known from quantitative LEED measurements [16] is a Si adatom structure with one adatom per (2×2) unit cell. The next structure is a model originally proposed as a Si rich structure for the *6H*-SiC(0001)-(3×3) reconstruction by Kulakov, Henn, and Bullemer [17], labeled *c*. In this model dangling bond saturation is optimal with only one out of nine dangling bonds per (3×3) cell remaining. Li and Tsong proposed a Si or C rich tetrahedrally shaped cluster as adatoms.[14] We tested different chemical combinations (Fig. 4 d *(i) -(iii)*). The surface energies of the originally proposed Si *(ii)* or C *(i)* rich and a plain Si *(ii)* cluster are given Fig. 2. In the main text, we included the most stable cluster formed by 4 Si atoms, labeled *d*.

On the basis of scanning tunneling microscope (STM) measurements Hoster, Kulakov, and Bullemer suggested a geometric configuration for the (3×3) reconstruction, however, the chemical composition was not specified.[11] We added a modification of the model, shown in Fig. 4 *e* for which we choose all adatoms to be Si. This is the most stable chemical composition that we tested of the Hoster *et al.* models. Hiebel *et al.* suggested a model consisting of a SiC-bilayer with a stacking fault of one half of the cell and two adatoms, a Si adatom and on the faulted side a C adatom, shown in Fig. 4 *f*.[12] The next structure, labeled *g*, is a carbon rich model suggested by Deretzis and La Magna. [13] It is a modification of model *e* with a change of the chemical composition to 6 C adatoms forming a dimer ring and 4 Si adatoms. Figure 4 *h* shows an additional variation of model *e*. This structure consist of a fractional bilayer with 7 Si adatoms bonded to the substrate and 3 C adatoms.

The density of states of the Si twist model

We here compare the spin-polarized and non spin polarized density of states (DOS) of the Si twist model. The results are similar to literature results reported for the $(\sqrt{3}\times\sqrt{3})$ Si-adatom reconstruction on the Si face of SiC [18]. Here, the unpolarized surface is by necessity metallic and the spin-polarization allows the surface to open a gap. This gap may well be due to a strong correlation effect, as discussed for the Si side by Rohlfing *et. al* [18] and references therein.

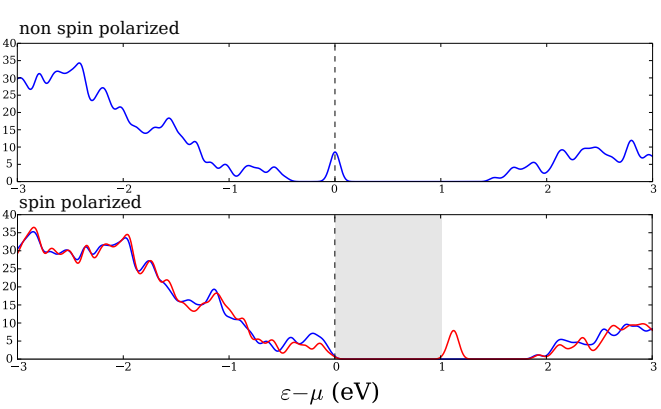

FIG. 3: The density of states (DOS) without spin polarization in the (upper panel) and spin polarized (lower panel). The unpolarized DOS is by necessity metallic, while the spin-polarized DOS clearly shows a band gap between the spin up and spin down states rendering the surface semiconducting.

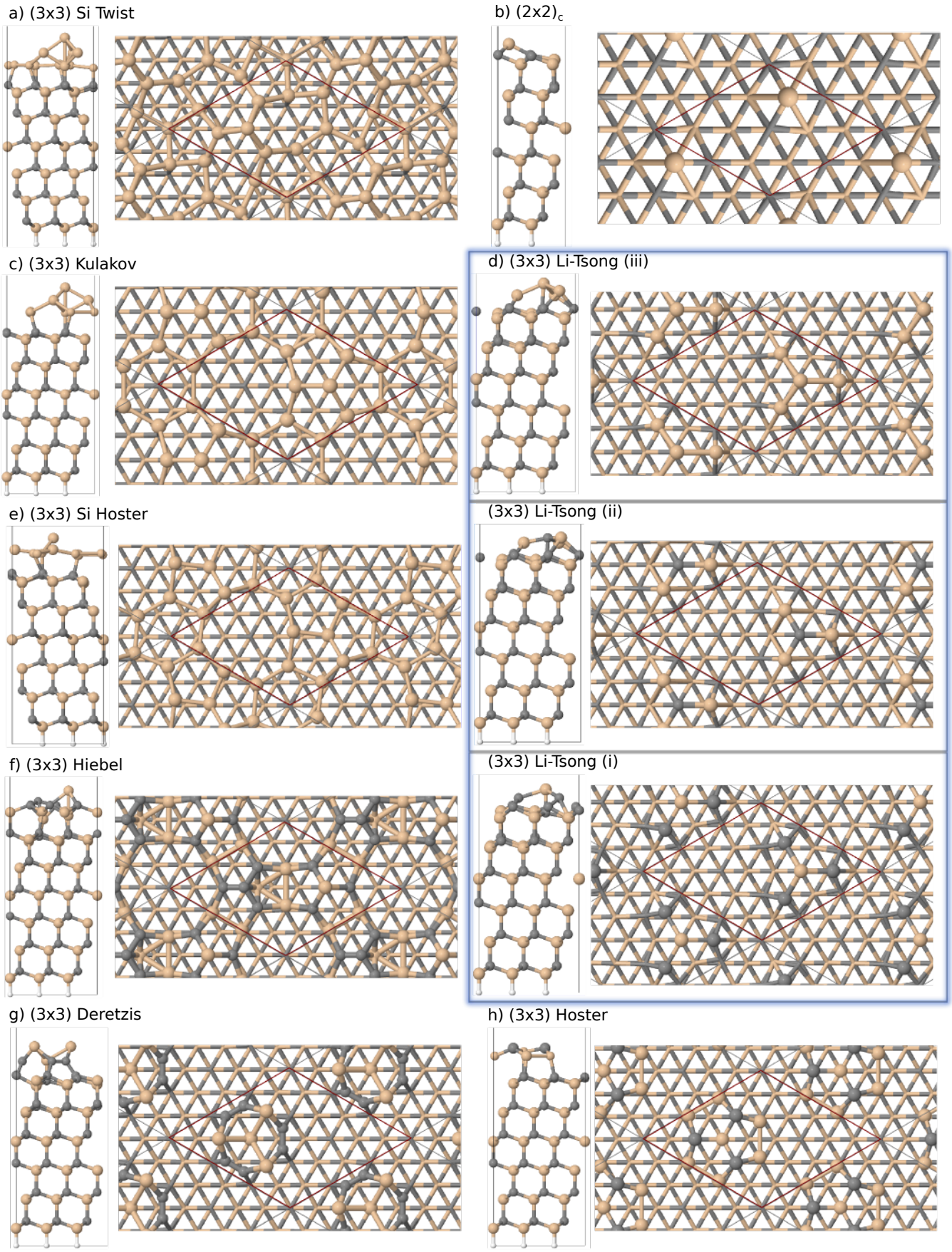

FIG. 4: All structural models for the (3×3) reconstructions of the *3C*-SiC($\bar{1}\bar{1}\bar{1}$) included in the surface energy diagram are shown in a side and top view. In the top view the unit cell is marked in red. The first structure (a) - the Si twist model - has been adapted from the Si face [15] and is discussed in detail in the main paper. (b) shows the $(2\times2)_C$ reconstruction as known from quantitative LEED measurements (b)[16]. A model adapted from the Si face is shown in (c)[17]. Previously proposed structure models for the (3×3) reconstructions: (d) Ref. [14], (e) Ref. [11] - as a plain Si adatom structure, (f) Ref. [12], (g) Ref. [13] and (h) Ref. [11]]. The right panel show three different chemical composition of the (3×3) reconstructions suggested by Li and Tsong ((3x3) Li-Tsong *(i)* -*(iii)*), their energetics are shown in Fig. 2.

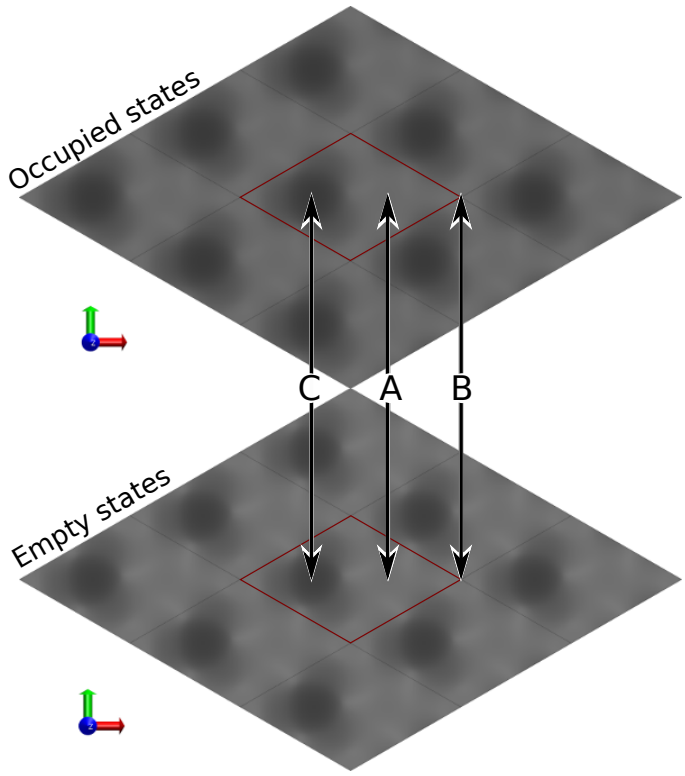

FIG. 5: Simulated constant current STM images are shown for the occupied and empty state of the Si twist model. The simulation were performed using the HSE06+vdW exchange correlation functional. The three points of interest (A, B, C) are marked by arrows and labeld according to Hiebel *et al.*[12]. Marked in red is the *3C*-SiC-(3×3) unit cell.

Simulated STM images of the Si twist model

Most of the previously proposed structure models for the *3C*-SiC($\bar{1}\bar{1}\bar{1}$)-(3×3) were motivated by STM measurements [11–13]. We here include simulated constant current STM images of the Si twist model Fig. 5.

The constant current STM images were obtained following the Tersoff-Hamann approach. [19, 20] In this approach, constant current images are approximated by an isosurface of the local density of states (l-DOS) integrated between the Fermi energy (ε_F) of the system and the tip bias (V_{tip}). We integrated the l-DOS on a real space grid with a resolution of 0.035 Å. The l-DOS was calculated using the Heyd-Scuseria-Ernzerhof hybrid functional (HSE06) at the PBE+vdW geometry.

In experiment, constant current STM images for the occupied and empty states show three pronounced signals. We chose the labeling with A, B and C according to Hiebel *et al.*[12] (see Fig.5), where point C is at the position of the top Si adatom. Feature B and C can be found in both the occupied and the empty states experimental images in agreement with our simulated images. However, in experiment feature A measured with a negative voltage differs from A measured with a positive voltage. This change in intensity is not observed in our simulated images. This could either be because of the crude approximation in the simulation of STM images or the model we propose is not the actually observed reconstruction.

* Present address: AQcomputare GmbH, Business Unit MATcalc, Annabergerstr. 240, 09125 Chemnitz, Germany

[1] V. Blum, R. Gehrke, F. Hanke, P. Havu, V. Havu, X. Ren, K. Reuter, and M. Scheffler, Comp. Phys. Commun. **180**, 2175 (2009).
[2] L. Nemec, V. Blum, P. Rinke, and M. Scheffler, Phys. Rev. Lett. **111**, 065502 (2013).
[3] A. V. Krukau, O. A. Vydrov, A. F. Izmaylov, and G. E. Scuseria, The Journal of Chemical Physics **125**, 224106 (2006).
[4] H. Hoechst, M. Tang, B. C. Johnson, J. M. Meese, G. W. Zajac, and T. H. Fleisch, Journal of Vacuum Science & Technology A **5**, 1640 (1987).
[5] R. Humphreys, D. Bimberg, and W. Choyke, Solid State Communications **39**, 163 (1981), ISSN 0038-1098.
[6] R. Ramprasad, H. Zhu, P. Rinke, and M. Scheffler, Phys. Rev. Lett. **108**, 066404 (2012).
[7] Z. Li and R. C. Bradt, Journal of Materials Science **21**, 4366 (1986).
[8] J. Harl and G. Kresse, Phys. Rev. Lett. **103**, 056401 (2009).
[9] J. Heyd, G. E. Scuseria, and M. Ernzerhof, The Journal of Chemical Physics **118**, 8207 (2003).
[10] H. Kleykamp, Berichte der Bunsengesellschaft für physikalische Chemie **102**, 1231 (1998).
[11] H. E. Hoster, M. A. Kulakov, and B. Bullemer, Surface Science **382**, L658 (1997).
[12] F. Hiebel, L. Magaud, P. Mallet, and J.-Y. Veuillen, Journal of Physics D: Applied Physics **45**, 154003 (2012).
[13] I. Deretzis and A. L. Magna, Applied Physics Letters **102** (2013).
[14] L. Li and I. S. T. Tsong, Surface Science **351**, 141 (1996).
[15] U. Starke, J. Schardt, J. Bernhardt, M. Franke, K. Reuter, H. Wedler, K. Heinz, J. Furthmüller, P. Käckell, and F. Bechstedt, Phys. Rev. Lett. **80**, 758 (1998).
[16] A. Seubert, J. Bernhardt, M. Nerding, U. Starke, and K. Heinz, Surface Science **454 – 456**, 45 (2000).
[17] M. Kulakov, G. Henn, and B. Bullemer, Surface Science **346**, 49 (1996).
[18] M. Rohlfing and J. Pollmann, Phys. Rev. Lett. **84**, 135 (2000).
[19] J. Tersoff and D. R. Hamann, Phys. Rev. Lett. **50**, 1998 (1983).
[20] J. Tersoff, Phys. Rev. B **40**, 11990 (1989).